



A New Structural-Dynamics Module for Offshore Multimember Substructures within the Wind Turbine Computer-Aided Engineering Tool FAST

Preprint

Huimin Song, Rick Damiani, Amy Robertson,
and Jason Jonkman

*Presented at the 23rd International Ocean, Offshore and Polar
Engineering Conference – ISOPE 2013
Anchorage, Alaska
June 30 – July 5, 2013*

**NREL is a national laboratory of the U.S. Department of Energy
Office of Energy Efficiency & Renewable Energy
Operated by the Alliance for Sustainable Energy, LLC.**

This report is available at no cost from the National Renewable Energy
Laboratory (NREL) at www.nrel.gov/publications.

Conference Paper
NREL/CP-5000-58093
August 2013

Contract No. DE-AC36-08GO28308

NOTICE

The submitted manuscript has been offered by an employee of the Alliance for Sustainable Energy, LLC (Alliance), a contractor of the US Government under Contract No. DE-AC36-08GO28308. Accordingly, the US Government and Alliance retain a nonexclusive royalty-free license to publish or reproduce the published form of this contribution, or allow others to do so, for US Government purposes.

This report was prepared as an account of work sponsored by an agency of the United States government. Neither the United States government nor any agency thereof, nor any of their employees, makes any warranty, express or implied, or assumes any legal liability or responsibility for the accuracy, completeness, or usefulness of any information, apparatus, product, or process disclosed, or represents that its use would not infringe privately owned rights. Reference herein to any specific commercial product, process, or service by trade name, trademark, manufacturer, or otherwise does not necessarily constitute or imply its endorsement, recommendation, or favoring by the United States government or any agency thereof. The views and opinions of authors expressed herein do not necessarily state or reflect those of the United States government or any agency thereof.

This report is available at no cost from the National Renewable Energy Laboratory (NREL) at www.nrel.gov/publications.

Available electronically at <http://www.osti.gov/bridge>

Available for a processing fee to U.S. Department of Energy and its contractors, in paper, from:

U.S. Department of Energy
Office of Scientific and Technical Information
P.O. Box 62
Oak Ridge, TN 37831-0062
phone: 865.576.8401
fax: 865.576.5728
email: <mailto:reports@adonis.osti.gov>

Available for sale to the public, in paper, from:

U.S. Department of Commerce
National Technical Information Service
5285 Port Royal Road
Springfield, VA 22161
phone: 800.553.6847
fax: 703.605.6900
email: orders@ntis.fedworld.gov
online ordering: <http://www.ntis.gov/help/ordermethods.aspx>

Cover Photos: (left to right) photo by Pat Corkery, NREL 16416, photo from SunEdison, NREL 17423, photo by Pat Corkery, NREL 16560, photo by Dennis Schroeder, NREL 17613, photo by Dean Armstrong, NREL 17436, photo by Pat Corkery, NREL 17721.



Printed on paper containing at least 50% wastepaper, including 10% post consumer waste.

A New Structural-Dynamics Module for Offshore Multimember Substructures within the Wind Turbine Computer-Aided Engineering Tool FAST

Huimin Song, Rick Damiani, Amy Robertson, Jason Jonkman
National Renewable Energy Laboratory
Golden, CO, USA

ABSTRACT

FAST, developed by the National Renewable Energy Laboratory, is a computer-aided engineering tool for aero-hydro-servo-elastic analysis of land-based and offshore wind turbines. This paper discusses the development of a new module (SubDyn), which when integrated to FAST, will enable loads simulations of offshore wind turbines with fixed-bottom, multimember support structures. The main theory and strategies for the implementation of the multimember substructure dynamics module (SubDyn) within the new FAST modularization framework are introduced. SubDyn relies on two main engineering schematizations: (1) a linear frame finite-element beam model (LFEB), and (2) a dynamics system reduction via Craig-Bampton's method. To test the SubDyn module and preliminarily assess the results against results from a commercial finite-element code, we analyzed a jacket support structure on its own and as part of an offshore system supporting a 5-MW turbine. The preliminary results show good agreement between the two codes.

KEY WORDS: Offshore; wind turbine; multimember; support structure; beam finite element; dynamic reduction; state space.

INTRODUCTION

Recently, there has been significant interest in offshore turbine support structures. Wind turbines are being placed further offshore because of the better wind resource, scarcity of land available for development, and reduced visual impact. The United States alone possesses large and accessible offshore wind resources that can provide a considerable amount of electricity-generating capacity. In fact, the National Renewable Energy Laboratory (NREL) estimates that the U.S. offshore winds have a gross potential capacity that is four times greater than the nation's present electric capacity (Musial and Ram, 2010). Additionally, different geographic locations require different support structure designs. In shallow water, where the water depth is less than 30 meters (m), monopiles and gravity-based substructures that extend to the seabed may be used. However, at transitional water depths of 30 to 60 m, monopiles are no longer economical and may exceed the manufacturing limit. As a result, fixed-bottom, multimember support structures such as jackets and tripods may be used (for water depth that

is greater than 60 m, floating platforms may be required). This paper focuses on the analysis of support structures commonly used in transitional water depths.

Many tools have been developed to analyze offshore wind turbines with jacket type support structures. FAST is one such tool. Developed by NREL, FAST is a computer-aided engineering (CAE) tool for aero-hydro-servo-elastic analysis of land-based and offshore wind turbines. Previously, FAST only had the capability of examining land-based and offshore wind turbines that were placed on either floating hulls or monopile substructures. But recent modifications made to FAST—through an updated platform hydrodynamics module (HydroDyn) (Song et al., 2012)—provide new capabilities to model the hydrodynamic loading that is imparted to the offshore multimember supports by waves and currents. This paper focuses on further efforts to enable the modeling of multimember structures in FAST, specifically, the development of structural-dynamics modeling of multimember support structures. In particular, we introduce the main theory and strategies used to implement SubDyn, the new multimember substructure dynamics module within FAST. SubDyn relies on a linear frame finite-element beam model (LFEB) that has the option of using a dynamics system reduction via the Craig-Bampton method.

LFEB can accommodate different element types, including Euler-Bernoulli and Timoshenko beam elements (the latter account for shear deformation and are better suited to represent low aspect ratio beams that may be used within frames and to transfer the loads within the frame) of either constant or longitudinally tapered cross sections. A previous study by Damiani et al. (2013a) has shown that linear theory yields acceptable results when analyzing wind turbine substructures. The large number of degrees-of-freedom ($\sim 10^3$) associated with a standard finite-element analysis of a typical multimember structure would hamper computational efficiency during wind turbine system dynamic simulations. As a result, for this study, we implemented a Craig-Bampton system reduction to speed up processing time while retaining a high level of fidelity in the overall system response.

NREL has recently put considerable effort into improving the overall modularity of FAST (Jonkman 2013a). The SubDyn module developed and presented in this paper will become a new module that can be

integrated into the FAST modularization framework through loose or tight coupling (including full-system linearization), thereby allowing simulations of offshore wind turbine systems in transitional water depths under combined wind, wave, and current loading, and including hydro-elastic effects. In the new FAST framework, the SubDyn module is called by the FAST driver program. In a loosely coupled time-integration scheme, the FAST driver program transfers data such as hydrodynamic forces, substructure responses, loads transmitted to the transition piece, and transition piece responses among the SubDyn, HydroDyn, and ElastoDyn (a structural (elastic) dynamics module that models the tower, rotor, nacelle, drivetrain, and the transition piece) modules at each time step. Within this scheme, SubDyn tracks its states and integrates its equations through its own solver. In a tightly coupled time-integration scheme, SubDyn sets up its own equations, but its states and those of other modules are tracked and integrated by a solver that is common to all of the modules.

SubDyn may also be used as a stand-alone module to analyze the substructure independently from the rest of the wind turbine system. In addition, SubDyn, as a substructure finite-element analysis module, is being integrated inside the jacket sizing tool (Damiani and Song, 2013b) within the NREL wind energy systems engineering initiative.

In this study, a jacket substructure both on its own and as part of a 5-MW offshore wind system were analyzed to test SubDyn's substructure integration with the transition piece, tower, and rotor-nacelle/assembly (RNA), and to preliminarily assess the results against the commercial software ANSYS (ANSYS, 2011). For this assessment, the natural frequencies and static deflections were computed for the jacket and the simplified turbine system. Preliminary verification of the results was performed against results from ANSYS models.

The paper layout is as follows. First we introduce the SubDyn module within the FAST modularization framework and its relation with other modules. Second, we introduce the SubDyn main theory including the LFE and the dynamic reduction using the Craig-Bampton method. The state-space formulations that are to be used in the time-domain simulation are then introduced. Finally, two examples are presented to show the preliminary results of the SubDyn module.

SUBDYN WITHIN THE FAST MODULARIZATION FRAMEWORK

NREL's core CAE tool, FAST (Jonkman and Buhl, 2005, Jonkman, 2013b) is based on advanced engineering models, derived from fundamental laws of physics, but with appropriate simplifications and assumptions, and supplemented with computational solutions and test data (where applicable).

FAST joins AeroDyn (a rotor aerodynamics module) (Laino and Hansen, 2002; Moriarty and Hansen, 2005); HydroDyn (Jonkman, 2007, 2009; Song et al., 2012) for offshore systems; SubDyn; ServoDyn (a control and electrical system (servo) dynamics module); and ElastoDyn to enable coupled nonlinear aero-hydro-servo-elastic analysis in the time domain. The FAST tool allows users to analyze a wide range of wind turbine configurations, including two- or three-bladed horizontal-axis rotors, pitch or stall regulation, rigid or teetering hubs, upwind or downwind rotors, and lattice or tubular towers. The wind turbine can be modeled on land or offshore on fixed-bottom or floating substructures.

NREL has recently put considerable effort into improving the overall modularity of FAST to enhance its ability to read, implement, and

maintain source code; increase module sharing and shared code development across the wind community; enrich numerical performance and robustness; and greatly enhance flexibility and expandability to enable further developments of functionality without the need to re-code established modules (Jonkman, 2013a). The new FAST modularization framework supports module-independent inputs, outputs, states, and parameters; states in continuous-time, discrete-time, and in constraint form; loose and tight coupling; independent time and spatial discretizations; time marching, operating-point determination, and linearization; data encapsulation; dynamic allocation; and save/retrieve capabilities. One of the benefits of a modular framework is that it allows modules to be interchanged, which can be important for benchmarking, research, and industrial applications because the required model fidelity is reliant on the application.

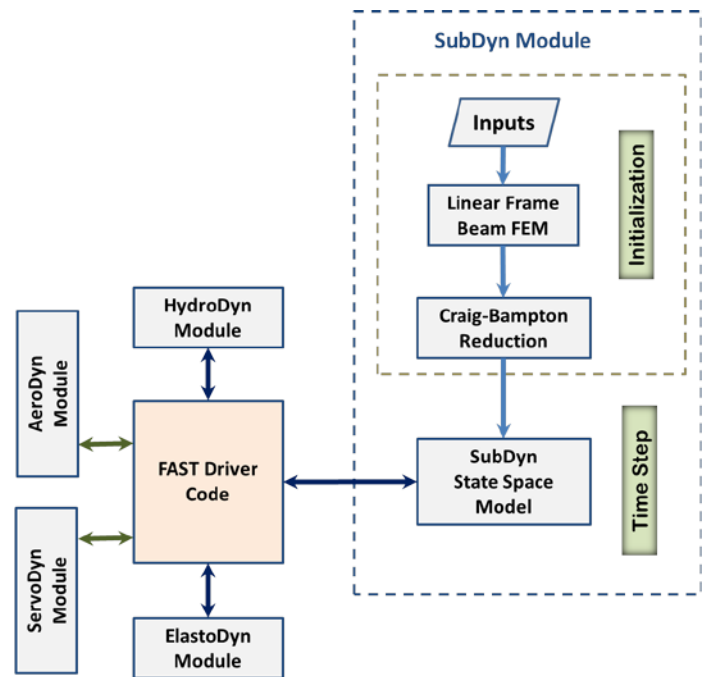


Fig. 1: SubDyn layout.

SubDyn is a substructure finite-element module for analyzing multimember substructure static and dynamic responses. The substructure is considered to be clamped at the seabed and rigidly connected to the transition piece at the substructure top nodes (interface nodes). Other restraints can be implemented via the input file, with a soil-pile interaction module intended for the future. When integrated with FAST, loads and responses are transferred between SubDyn, HydroDyn, and ElastoDyn via the FAST driver program. At the interface nodes, the transition piece displacement, rotation, velocity, and acceleration are inputs from the ElastoDyn module and the reaction forces at the transition piece are outputs of the SubDyn module. SubDyn also outputs the substructure displacements and velocities to the HydroDyn module to calculate the hydrodynamic forces that are inputs for the SubDyn module. In addition, the SubDyn module can calculate the member forces, as requested by the user. Figure 1 shows the basic layout of the SubDyn module.

The input file defines the substructure geometry, material properties, and constraints. Users can define element types; full finite-element mode or Craig-Bampton reduction; the number of modes to be retained in the Craig-Bampton reduction; modal damping coefficients; and the number of elements for each member.

SubDyn relies on two main engineering schematizations: (1) a linear frame finite-element beam model (LFEB), and (2) a dynamics system reduction via Craig-Bampton's method.

Nonlinearities come from many aspects, including material nonlinearity, axial shortening due to bending, large displacement, and so on. The material nonlinearity is not considered here because most of the offshore multimember support structures are designed to use steel and the maximum stress is intended to be below the yield strength of the material. Damiani et al. (2013a) showed that a linear finite-element method was suitable when analyzing wind turbine substructures, in which several wind turbine configurations that varied in base geometry, load paths, sizes, supported towers, and turbine masses were analyzed under extreme loads using nonlinear and linear models. The results revealed that the nonlinear behavior was mainly caused by the mono-tower response and had little effect on the multimember support structures. Therefore, an LFEB model for the substructure was considered appropriate within the FAST modularization framework.

The dynamic analysis of the wind turbine system requires numerous time-step calculations. Yet, the large number of degrees of freedom (DOF) associated with a standard finite-element analysis of a typical multimember structure could hamper computational efficiency during wind turbine system dynamic simulations. Therefore, a Craig-Bampton methodology is used to re-characterize the substructure finite-element model into a reduced DOF model that maintains the fundamental low-frequency response modes of the structure. In the FAST initialization step, SubDyn reduces the large substructure physical degrees of freedom (displacements) to a small number of modal DOFs and interface (boundary) DOFs, and during each time step, only these DOFs and associated velocities need to be calculated.

The state-space formulation sets the equation of motion of the substructure system with physical DOFs at the interface and modal DOFs representing all interior motions. At each time step, loads are exchanged between modules through the driver code; the modal responses are calculated inside the SubDyn state-space model; and the next time-step responses are calculated by the SubDyn integrator for loose coupling and the system integrator for tight coupling.

LINEAR FRAME FINITE-ELEMENT BEAM MODEL

In SubDyn, the LFEB can accommodate different two-node beam element types, including Euler-Bernoulli and Timoshenko beam elements, either of constant or tapered cross sections. The uniform and tapered Euler-Bernoulli beam elements are displacement-based and use third-order interpolation functions that guarantee the displacement and rotation continuity between elements. The uniform Timoshenko beam element is derived by introducing the shear deformation into the uniform Euler-Bernoulli element, so the displacements are represented by third-order interpolation functions as well. For the two-node-tapered Timoshenko element, the displacements and rotations are represented using first-order interpolation functions, respectively. Therefore, when the beam element is thin, the low-order displacement representation will result in very stiff behavior (also known as shear locking). To minimize the shear-locking effects when using two-node Timoshenko tapered elements, we recommend applying reduced integration or a fine discretization, or applying three-node- or four-node-tapered elements where the displacements are represented by higher order interpolation functions. Currently, only a two-node-tapered Timoshenko element is provided; three- or four-node-tapered Timoshenko elements will be implemented in the future.

Many researchers have presented theories on finite-element formulation on tapered Timoshenko beams, such as Greenhill et al. (1985), Hinnant (1989), and Rao and Gupta (2001). In their research, bending stiffness was considered to change only through the section geometry along the beam axis. In other words, for a homogeneous, isotropic-tapered beam, the bending stiffness EI is simply written as $EI(x)$, where I varies along the axis of the beam due to the taper. Many recent studies follow the same methodology, such as Abdel-Jaber et al. (2008), Das et al. (2009), and De Rosa et al. (2010), where the bending strain energy is simply written as $EI(x)\kappa^2/2$. In this paper, the tapered beam elements were developed following the same methodology and only for circular cross-section beam elements.

However, Hodges et al. (2008, 2010) pointed out that the bending stiffness depends on the taper, which leads to bending and shear coupling for a tapered beam with rectangular cross sections. As a result, correction factors are required for the bending stiffness when computing the strain energy, and the effect of correction factors is found to be significant, especially for deep beams. There is no research that shows the effect of taper on circular cross sections and further research is needed to assess the correction factors for bending stiffness associated with circular cross sections. This type of research will be considered in a future investigation.

DYNAMIC SYSTEM REDUCTION

The dynamic analysis of a wind turbine system requires numerous time-step calculations. For the multimember structure, the number of DOFs can be in the thousands, thereby hampering the computational efficiency of wind turbine system dynamic simulations. A typical wind turbine system model in FAST has about 20 DOFs. Therefore, a Craig-Bampton methodology is used to re-characterize the substructure finite-element model into a reduced DOF model that maintains the fundamental low-frequency response modes of the structure. With the Craig-Bampton method, the DOFs of the substructure can be reduced to about 10 (user defined). This system reduction method was first introduced by Hurty (1964) and later expanded by Craig and Bampton (1968).

In SubDyn's Craig-Bampton reduction, the structure nodes are separated into two groups: (1) the boundary nodes that include the constrained boundary and interface nodes, and (2) the rest of the nodes. The constrained boundary nodes are the nodes that are constrained at the seabed, the interface nodes are the nodes connected to the transition piece, and the remaining nodes are labeled as interior nodes.

The fundamental assumption of the Craig-Bampton method is that the contribution to the displacement of the interior nodes can be approximated by only a subset of the interior generalized DOFs. This reduced basis is chosen as the first few eigenvectors that are arranged by increasing eigenfrequencies.

The Craig-Bampton method is used to obtain the reduced mass, damping, and stiffness matrices of the substructure. Then, in loose coupling, the current time-step response of the substructure can be obtained through the processing of the instantaneous loads by HydroDyn and the transition piece motion by ElastoDyn, including the known SubDyn states (these states are discussed in the next section). The next time-step modal DOFs can be obtained using an integrator within SubDyn. In tight coupling, the response will be obtained by an integrator that is common to all modules.

The derivation of the system reduction is as follows. After the LFEB assembly, the system equation of motion can be partitioned as follows:

$$\begin{bmatrix} M_{RR} & M_{RL} \\ M_{LR} & M_{LL} \end{bmatrix} \begin{Bmatrix} \dot{U}_R \\ \dot{U}_L \end{Bmatrix} + \begin{bmatrix} C_{RR} & C_{RL} \\ C_{LR} & C_{LL} \end{bmatrix} \begin{Bmatrix} \dot{U}_R \\ \dot{U}_L \end{Bmatrix} + \begin{bmatrix} K_{RR} & K_{RL} \\ K_{LR} & K_{LL} \end{bmatrix} \begin{Bmatrix} U_R \\ U_L \end{Bmatrix} = \begin{Bmatrix} F_R + F_{Rg} \\ F_L + F_{Lg} \end{Bmatrix} \quad (1.0)$$

Where M , C , and K are mass, damping, and stiffness matrices, respectively; and U and F are nodal DOFs and applied forces, respectively. A derivative with respect to time is represented by a dot, so that \dot{U} is the derivative of U . Note that the applied forces include the hydrodynamic forces from HydroDyn (F_R, F_L) and gravity forces (F_{Rg}, F_{Lg}), which are considered as static forces that are lumped at each node. The subscript R stands for the restrained DOFs, which include the constrained DOFs at the seabed and the interface DOFs connected to the transition piece. The subscript L stands for all of the interior DOFs. Typically, the term C_{LL} is the only nonzero term in the damping matrix.

By using the Craig-Bampton transformation, the interior DOFs are transformed from physical DOFs to modal DOFs:

$$\begin{bmatrix} M_{BB} & M_{Bm} \\ M_{mB} & I \end{bmatrix} \begin{Bmatrix} \dot{U}_R \\ \dot{q}_m \end{Bmatrix} + \begin{bmatrix} 0 & 0 \\ 0 & 2\zeta\Omega_m \end{bmatrix} \begin{Bmatrix} \dot{U}_R \\ \dot{q}_m \end{Bmatrix} + \begin{bmatrix} K_{BB} & 0 \\ 0 & \Omega_m^2 \end{bmatrix} \begin{Bmatrix} U_R \\ q_m \end{Bmatrix} = \begin{Bmatrix} (F_R + F_{Rg}) + \Phi_R^T (F_L + F_{Lg}) \\ \Phi_m^T (F_L + F_{Lg}) \end{Bmatrix} \quad (1.1)$$

where q_m are the reduced modal DOFs according to the m number of modes retained (provided by the user). Ω_m is the diagonal matrix containing the frequencies corresponding to the m lowest interior modes Φ_m . The diagonal matrix that contains the modal damping coefficients corresponding to each retained internal mode is ζ . And Φ_R represents constrained modes.

The internal modes, Φ_L , are obtained by solving the eigenvalue problem:

$$K_{LL}\Phi_L = \omega^2 M_{LL}\Phi_L \quad (1.2)$$

and Φ_L is selected so that $\Phi_L^T M_{LL} \Phi_L = I$ (mass normalized), where I is the identity matrix. Φ_m is the truncated set of Φ_L (keeping m of the total modes), and Ω_m contains the corresponding eigenfrequencies.

The restrained modes, Φ_R , are calculated as:

$$\Phi_R = -K_{LL}^{-1} K_{LR} \quad (1.3)$$

The matrix partitions in Eq. (1.1) are calculated as follows:

$$\begin{aligned} M_{BB} &= M_{RR} + M_{RL}\Phi_R + \Phi_R^T M_{LR} + \Phi_R^T M_{LL} \Phi_R \\ M_{mB} &= \Phi_m^T M_{LR} + \Phi_m^T M_{LL} \Phi_R \\ M_{Bm} &= M_{mB}^T \\ K_{BB} &= K_{RR} + K_{RL}\Phi_R \end{aligned} \quad (1.4)$$

The substructure interface nodes are rigidly connected to the transition piece, which is presently considered as a rigid block, so it is convenient to use the transition piece DOFs (one node with 6 DOFs at the reference point of the transition piece) in place of the interface DOFs.

The interface DOFs, \bar{U}_R , and the transition piece DOFs are related as follows:

$$\bar{U}_R = T_i U_{TP} \quad (1.5)$$

where T_i is a $(6 \cdot NIN) \times 6$ matrix, NIN is the number of interface nodes, and U_{TP} is the 6 DOFs of the rigid transition piece. Matrix T_i can be written as follows:

$$T_i = \begin{bmatrix} 1 & 0 & 0 & 0 & \Delta Z_1 & -\Delta Y_1 \\ 0 & 1 & 0 & -\Delta Z_1 & 0 & \Delta X_1 \\ 0 & 0 & 1 & \Delta Y_1 & -\Delta X_1 & 0 \\ 0 & 0 & 0 & 1 & 0 & 0 \\ 0 & 0 & 0 & 0 & 1 & 0 \\ 0 & 0 & 0 & 0 & 0 & 1 \\ \vdots & \vdots & \vdots & \vdots & \vdots & \vdots \\ 1 & 0 & 0 & 0 & \Delta Z_i & -\Delta Y_i \\ 0 & 1 & 0 & -\Delta Z_i & 0 & \Delta X_i \\ 0 & 0 & 1 & \Delta Y_i & -\Delta X_i & 0 \\ 0 & 0 & 0 & 1 & 0 & 0 \\ 0 & 0 & 0 & 0 & 1 & 0 \\ 0 & 0 & 0 & 0 & 0 & 1 \\ \vdots & \vdots & \vdots & \vdots & \vdots & \vdots \end{bmatrix}, \quad (i=1,2,\dots,NIN) \quad (1.6)$$

where

$$\begin{aligned} \Delta X_i &= X_{iNi} - X_{TP} \\ \Delta Y_i &= Y_{iNi} - Y_{TP} \\ \Delta Z_i &= Z_{iNi} - Z_{TP} \end{aligned} \quad (1.7)$$

where $(X_{iNi}, Y_{iNi}, Z_{iNi})$ is the coordinate of i^{th} interface node and (X_{TP}, Y_{TP}, Z_{TP}) is the coordinate of the transition piece reference point within the global coordinate system.

In terms of the transition piece DOFs, the system equation of motion (1.1) after the boundary constraints are applied (the DOFs of the nodes that are restrained at the seabed are removed from the equation of motion) becomes:

$$\begin{bmatrix} \tilde{M}_{BB} & \tilde{M}_{Bm} \\ \tilde{M}_{mB} & I \end{bmatrix} \begin{Bmatrix} \dot{U}_{TP} \\ \dot{q}_m \end{Bmatrix} + \begin{bmatrix} 0 & 0 \\ 0 & 2\zeta\Omega_m \end{bmatrix} \begin{Bmatrix} \dot{U}_{TP} \\ \dot{q}_m \end{Bmatrix} + \begin{bmatrix} \tilde{K}_{BB} & 0 \\ 0 & \Omega_m^2 \end{bmatrix} \begin{Bmatrix} U_{TP} \\ q_m \end{Bmatrix} = \begin{Bmatrix} \tilde{F}_{TP} \\ \tilde{F}_m \end{Bmatrix} \quad (1.8)$$

with

$$\begin{aligned} \tilde{M}_{BB} &= T_i^T \bar{M}_{BB} T_i \\ \tilde{M}_{Bm} &= T_i^T \bar{M}_{Bm} \\ \tilde{M}_{mB} &= \bar{M}_{mB}^T \\ \tilde{K}_{BB} &= T_i^T \bar{K}_{BB} T_i \\ \tilde{F}_{TP} &= F_{TP} + T_i^T \bar{F}_{Rg} + T_i^T \bar{\Phi}_R^T (F_L + F_{Lg}) \\ \tilde{F}_m &= \Phi_m^T (F_L + F_{Lg}) \end{aligned} \quad (1.9)$$

where the overhead bar stands for the matrices/vectors after the boundary conditions are applied, and $F_{TP} = T_i^T \bar{F}_R$ is the transition piece reaction force. Equation (1.8) is the equation of motion of the substructure after the Craig-Bampton reduction. The total DOFs of the substructure are reduced from $(6 \times \text{total number of nodes})$ to $(6 + m)$.

During the FAST initialization, the driver program calls the SubDyn initialization where the parameter matrices \tilde{M}_{BB} , \tilde{M}_{mB} , \tilde{M}_{Bm} , \tilde{K}_{BB} , Φ_m , Φ_R , T_I , the arrays \bar{F}_{Rg} and F_{Lg} , and the internal frequency matrix Ω_m are calculated. The substructure responses at each time step can then be obtained by using the state-space formulation discussed below.

STATE-SPACE FORMULATION

The substructure responses at each time step are represented by state-space formulations when integrated within the FAST framework. The state-space formulation of substructure dynamic systems can be developed in terms of inputs, outputs, states, and parameters. The notations highlighted here are consistent with those used in Jonkman (2013a). Inputs (identified by u) are a set of values supplied to SubDyn, and, along with the states, are needed to calculate future states and the system's output. Outputs (y) are a set of values calculated by and returned from SubDyn that depend on the states, inputs, and/or parameters through output equations (with functions Y). States are a set of internal values of SubDyn that are influenced by inputs and used to calculate future state values and the output. In SubDyn, only continuous states are considered. Continuous states (x) are states that are differentiable in time and characterized by continuous time differential equations (with functions X). Parameters (p) are a set of internal system values that are independent of the states and inputs. Furthermore, parameters can be fully defined at initialization and characterize a system's state equations and output equations.

In SubDyn, the inputs are defined as:

$$u = \begin{Bmatrix} u_1 \\ u_2 \\ u_3 \\ u_4 \end{Bmatrix} = \begin{Bmatrix} U_{TP} \\ \dot{U}_{TP} \\ \ddot{U}_{TP} \\ F_L \end{Bmatrix} \quad (1.10)$$

where F_L are the hydrodynamic forces on every interior node of the substructure from HydroDyn; U_{TP} , \dot{U}_{TP} , and \ddot{U}_{TP} are transition piece deflections (6 DOFs), velocities, and accelerations, respectively.

In first-order form, the states are defined as:

$$x = \begin{Bmatrix} x_1 \\ x_2 \end{Bmatrix} = \begin{Bmatrix} q_m \\ \dot{q}_m \end{Bmatrix} \quad (1.11)$$

From the system equation of motion, the state equation can be written as a standard linear system state equation:

$$\dot{X} = Ax + Bu + F_x \quad (1.12)$$

where

$$A = \begin{bmatrix} 0 & I \\ -\Omega_m^2 & -2\zeta\Omega_m \end{bmatrix}, \quad B = \begin{bmatrix} 0 & 0 & 0 & 0 \\ 0 & 0 & -\tilde{M}_{mB} & \Phi_m^T \end{bmatrix}, \quad F_x = \begin{Bmatrix} 0 \\ \Phi_m^T F_{Lg} \end{Bmatrix}$$

In SubDyn, the outputs to the ElastoDyn module are the reaction forces at the transition piece F_{TP} :

$$y_1 = -F_{TP} \quad (1.13)$$

The output equation for y_1 can be found as:

$$-Y_1 = C_1 x + D_1 u + F_Y \quad (1.14)$$

where

$$C_1 = \begin{bmatrix} -\tilde{M}_{Bm}\Omega_m^2 & -2\tilde{M}_{Bm}\zeta\Omega_m \end{bmatrix}$$

$$D_1 = \begin{bmatrix} \tilde{K}_{BB} & 0 & \tilde{M}_{BB} - \tilde{M}_{Bm}\tilde{M}_{mB} & \tilde{M}_{Bm}\Phi_m^T - T_I^T\bar{\Phi}_R^T \end{bmatrix}$$

$$F_Y = \tilde{M}_{Bm}\Phi_m^T F_{Lg} - T_I^T(\bar{F}_{Rg} + \bar{\Phi}_R^T F_{Lg})$$

The outputs to HydroDyn and other modules are the deflections and velocities of the substructure:

$$y_2 = \begin{Bmatrix} \bar{U}_R \\ U_L \\ \dot{\bar{U}}_R \\ \dot{U}_L \end{Bmatrix} \quad (1.15)$$

The output equation for y_2 can be written as:

$$Y_2 = C_2 x + D_2 u \quad (1.16)$$

where

$$C_2 = \begin{bmatrix} 0 & 0 \\ \Phi_m & 0 \\ 0 & 0 \\ 0 & \Phi_m \end{bmatrix}$$

$$D_2 = \begin{bmatrix} T_I & 0 & 0 & 0 \\ \bar{\Phi}_R^T T & 0 & 0 & 0 \\ 0 & T_I & 0 & 0 \\ 0 & \bar{\Phi}_R^T T & 0 & 0 \end{bmatrix}$$

SubDyn can also calculate member forces by starting from the forces computed at the nodes of the elements that are contained in the member as:

$$\text{Element Inertia load: } F_I^e = M^e \ddot{U}^e \quad (1.17)$$

$$\text{Element Static load: } F_S^e = K^e U^e$$

where K^e and M^e are element stiffness and mass matrices, respectively. And U_e and \ddot{U}_e are element nodal deflections and accelerations respectively, which can be obtained from Eq. (1.15) and Eq. (1.18):

$$\begin{Bmatrix} \ddot{\bar{U}}_R \\ \ddot{U}_L \end{Bmatrix} = \bar{C}x + \bar{D}u + \bar{F} \quad (1.18)$$

where

$$\bar{C} = \begin{bmatrix} 0 & 0 \\ -\Phi_m\Omega_m^2 & -2\Phi_m\zeta\Omega_m \end{bmatrix}$$

$$\bar{D} = \begin{bmatrix} 0 & 0 & T_I & 0 \\ 0 & 0 & \bar{\Phi}_R^T T_I - \Phi_m\tilde{M}_{mB} & \Phi_m\Phi_m^T \end{bmatrix}$$

$$\bar{F} = \begin{Bmatrix} 0 \\ \Phi_m\Phi_m^T F_{Lg} \end{Bmatrix}$$

There is no good way to quantify the damping forces for each element, so the element damping forces are not calculated.

At time $t = 0$, $u(0)$ and $x(0)$ are specified as initial conditions. During each subsequent time step, the inputs and states are known values, where inputs $u(t)$ are data coming from the ElastoDyn module and HydroDyn module, and states $x(t)$ are calculated from previous time-step integration. All of the parameter matrices are calculated in the SubDyn module initiation. With known $u(t)$ and $x(t)$, $\dot{x}(t)$ can be calculated using the state equation $\dot{x}(t) = X(u, x, t)$, and the outputs $y_1(t)$ and $y_2(t)$ can be calculated using the output functions $Y_1(u, x, t)$ and $Y_2(u, x, t)$. The element forces can also be calculated using Eq. (1.17). The next time-step states $x(t + \Delta t)$ can be obtained by integration:

$$\begin{bmatrix} u(t), \dot{x}(t), x(t) \end{bmatrix} \xrightarrow{\text{Integrate}} x(t + \Delta t) \quad (1.19)$$

For loose coupling, each module will have its own integrator, whereas for tight coupling, the states from all the modules will be integrated simultaneously using an integrator that is common to all modules.

Currently, the state-space formulation is not implemented, but it will be integrated within the FAST modularization framework in the near future.

REACTION CALCULATION

The reactions at the base of the structure are the member forces at the base nodes. These are usually provided in member local reference frames. Additionally, the user may request an overall reaction \vec{R} (six forces and moments per Eq. (1.20)) lumped at the center of the structure (tower centerline) and mudline, i.e., at the reference point $(0, 0, -W_{depth})$ in the global reference frame, with W_{depth} denoting the water depth. \vec{R} is a six element array that can be calculated in matrix form as follows:

$$\vec{R} = \begin{bmatrix} F_x \\ \vdots \\ M_z \end{bmatrix} = T_{React} F_{React} \quad (1.20)$$

where F_{React} is a $(6N_{react})$ array containing the forces and moments at the N_{react} boundary nodes in global coordinate frame, and T_{React} is a $(6 \times 6N_{react})$ matrix, as follows:

$$\begin{bmatrix} 1 & 0 & 0 & 0 & 0 & 0 & 1 & 0 & 0 & 0 & 0 & 0 \\ 0 & 1 & 0 & 0 & 0 & 0 & 0 & 1 & 0 & 0 & 0 & 0 \\ 0 & 0 & 1 & 0 & 0 & 0 & 0 & 0 & 1 & 0 & 0 & 0 \\ 0 & -\Delta z_1 & \Delta y_1 & 1 & 0 & 0 & 0 & -\Delta z_{N_{react}} & \Delta y_{N_{react}} & 1 & 0 & 0 \\ \Delta z_1 & 0 & -\Delta x_1 & 0 & 1 & 0 & \Delta z_{N_{react}} & 0 & -\Delta x_{N_{react}} & 0 & 1 & 0 \\ -\Delta y_1 & \Delta x_1 & 0 & 0 & 0 & 1 & -\Delta y_{N_{react}} & \Delta x_{N_{react}} & 0 & 0 & 0 & 1 \end{bmatrix} T_{React} = \begin{bmatrix} F_x \\ \vdots \\ M_z \end{bmatrix} \quad (1.21)$$

where Δx_i , Δy_i , and Δz_i ($i=1..N_{react}$) are coordinates of the boundary nodes with respect to the reference point.

EXAMPLES AND RESULTS

Case 1: Modal Analysis of a Jacket Substructure

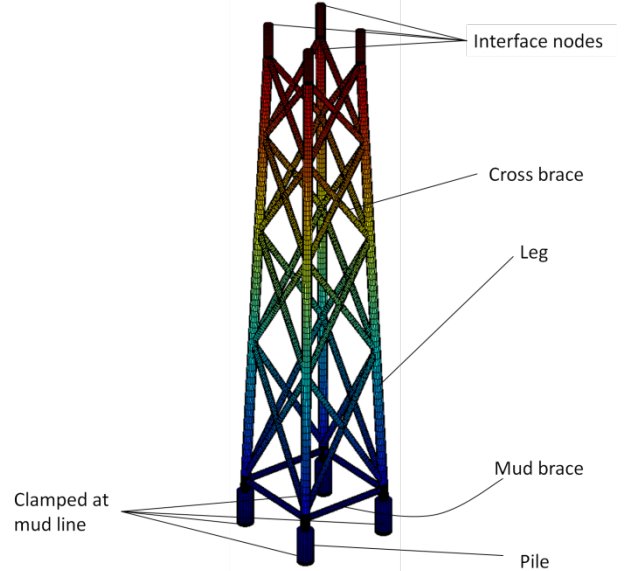


Fig. 2: Offshore Code Comparison Collaboration Continuation (OC4) jacket.

A jacket designed to support the NREL 5-megawatt (MW) reference turbine, as used in the International Energy Agency (IEA) Wind Task 30 Offshore Code Comparison Collaboration Continuation (OC4) research project, was analyzed using SubDyn. This support structure was originally designed by Vemula et al. (2010) for the UpWind Project. The design was adopted for the OC4 project at a water depth of 50 m (as shown in Fig. 2), and the structure was cantilevered at the mud line. The interface nodes were rigidly connected to the transition piece, which was modeled in this study as a massless point without inertia. The main geometric parameters of the jacket are provided in Table 1, but more details can be found in Vorpahl et al. (2011).

Table 1. OC4 jacket parameters

Parameter	Value
Leg outer diameter (OD) [m]	1.2
Leg thickness [m]	0.05 (up to the first bay)- 0.035–0.04 (transition piece)
Brace OD [m]	0.8
Brace thickness [m]	0.02
Pile OD [m]	2.082
Pile thickness [m]	0.6

The jacket support structure was modeled with SubDyn using full finite-element and Craig-Bampton's method (C-B), with a number of internal modes, as well as with ANSYS. Two-node, nontapered Timoshenko beam elements were used in all of the SubDyn models. The steel density was artificially augmented to $8,500 \text{ kg/m}^3$, namely to account for secondary steel not directly modeled. In the ANSYS model, each member was discretized into 10 beam elements (the number of elements was proven to not be a factor of the analysis results), and the top of the jacket was modeled as a rigid region using rigid constraints. For the SubDyn models, the connection to the transition piece was modeled using the transformation matrix to reduce the interface nodes to the transition piece reference point, as shown in Eq. (1.6). In the SubDyn full finite-element model, members were discretized into two

elements each, resulting in 1,014 DOFs. Multiple Craig-Bampton (C-B) reductions were performed within SubDyn to determine the sensitivity of the structural frequencies to the number of internal modes chosen. The SubDyn C-B calculations used 4, 8, and 12 internal modes for a total of 10, 14, and 18 DOFs, respectively.

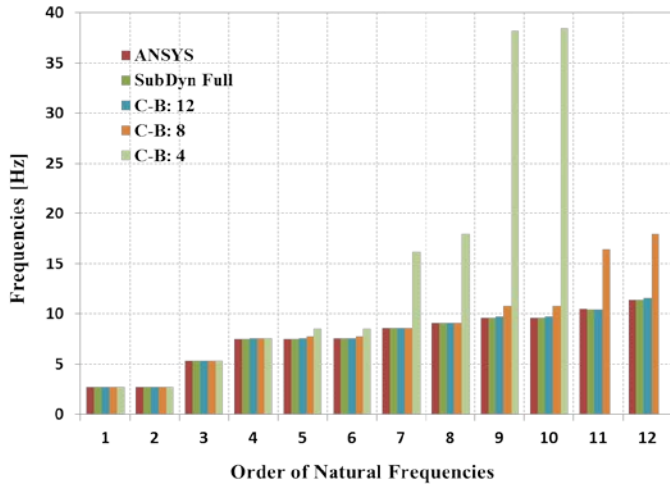


Fig. 3: Frequencies of the OC4 jacket using ANSYS and SubDyn.

Fig. 3 shows the lowest 12 natural frequencies of the OC4 jacket, as calculated by ANSYS, SubDyn full finite-element, and SubDyn C-B, with the different levels of modal reduction discussed above. Fig. 3 shows that the ANSYS and SubDyn full finite-element results matched very well. The slight difference in the 11th mode is caused by the different methods used by the two codes to treat the rigid connection at the interface nodes. By using SubDyn C-B, good results were achieved at low frequencies by using just a few internal modes, which will greatly accelerate the subsequent simulation time. The SubDyn results show that using only four internal modes provided fairly accurate approximations of the four lowest modes of the jacket structure. Increasing the number of internal modes improves the higher-frequency predictions. Because higher-frequency modes contribute little to the dynamic response to low-frequency forcing, a user can select the number of internal modes based on the forcing frequency range to reduce the number of substructure DOFs.

Case 2: Modal Analysis and Static Response of a Wind Turbine System

The support structure in Case 1 was then incorporated into a full offshore wind system by placing the NREL 5-MW turbine and tower atop the OC4 jacket substructure (see also Fig. 4). This system was then studied to test SubDyn’s ability to accurately represent the

eigenfrequencies and static response of a turbine system. Static analyses were performed under two rotor thrust loads [2,000 and 4,000 (kN) in magnitude] applied at the assumed RNA center of mass (CM) and directed along the horizontal x-axis. Additionally, the influence of the RNA self-weight and the jacket self-weight were considered in SubDyn. The tower, transition piece, RNA mass, and trust parameters are listed in Table 2.

Table 2. Tower geometric, inertial, and thrust parameters

Parameter	Value
Deck height above mean sea level (MSL) [m]	16
Transition-piece length [m]	4
Tower-base OD [m]	5.6
Tower-base thickness [m]	0.032
Tower-top OD [m]	4
Tower-top thickness [m]	0.03
Tower length [m]	68
RNA vertical offset [m]	2.34
Turbine hub height [m]	90
RNA mass [ton]	350
Jacket mass [ton]	581+(427 pile/grout)
Transition piece mass [ton]	666
Tower mass [ton]	230
Thrust [kN]	2,000 and 4,000

In the ANSYS model, five pipe elements were utilized per jacket member, and 20 tapered beam elements were used for the tower. According to the analysis results, the number of elements proved to not be a factor. For the SubDyn full finite-element model, we used 80 elements for the tower and 258 elements for the remainder of the jacket structure. For the SubDyn C-B models, we used a driver code to call SubDyn to run a full finite-element analysis of the tower, RNA, and transition piece, and then SubDyn was called to run a C-B reduction analysis of the jacket substructure. The matrices were subsequently assembled by the driver code to obtain results of the whole system. Eighty elements were used for the tower and various numbers of jacket internal modes were used for different cases. The tower, RNA, and transition piece models were assembled with the jacket substructure model at the interface, which was the transition piece reference point. For all of the models, the RNA was considered as a point mass (rotational inertia was ignored) and located at the RNA center of mass. In all cases, the transition piece was considered as a concentrated mass with inertia that was located at the transition piece reference point. The maximum relative error in calculated mass between the ANSYS and SubDyn models was less than 0.06%. The added mass was not included in the current models, but in the final FAST framework, the added mass will be transmitted to SubDyn at each time step from HydroDyn.

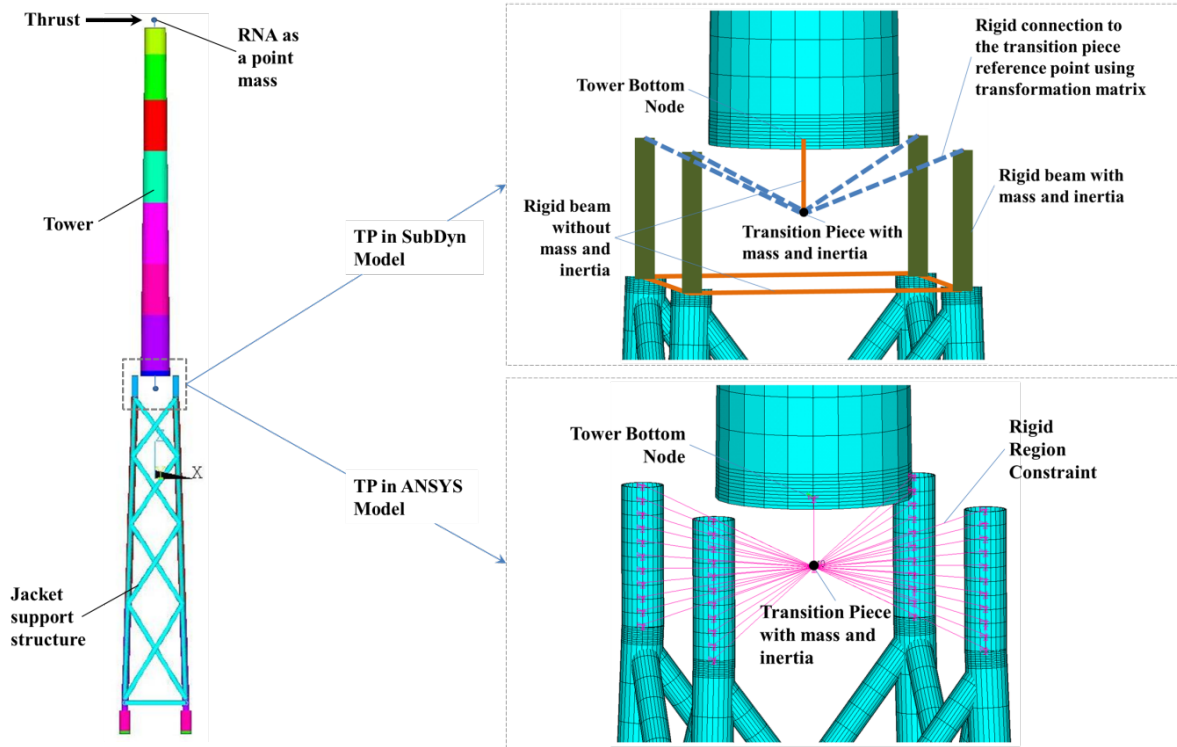


Fig. 4: OC4 wind turbine system and transition piece models.

Table 3. Natural frequencies of the OC4 wind turbine system [Hz]

Mode No.	ANSYS Full FEM	SubDyn				
		Full FEM	CB: 12	CB: 8	CB: 4	CB: 1
1	0.3190	0.3190	0.3190	0.3190	0.3190	0.3190
2	0.3190	0.3190	0.3190	0.3190	0.3190	0.3190
3	1.1936	1.1944	1.1945	1.1945	1.1947	1.1947
4	1.1936	1.1944	1.1945	1.1945	1.1947	1.1951
5	3.4425	3.3738	3.3803	3.3803	3.4211	3.4211
6	4.1253	4.1288	4.1321	4.1322	4.1375	4.1377
7	4.1253	4.1292	4.1323	4.1325	4.1378	4.1862
8	5.3391	5.3417	5.3480	5.3497	5.3523	5.3523
9	6.6953	6.6991	6.7020	6.7027	6.7088	6.7096
10	6.6953	6.7016	6.7038	6.7034	6.7103	9.5861

The natural frequencies of the OC4 wind turbine system are listed in Table 3; Fig. 5 shows the first 6 eigenfrequencies in graphical format. The results are from the different models—the ANSYS full FEM, the SubDyn full FEM, and the SubDyn C-B—with substructure reduction using 1, 4, 8, and 12 internal modes.

From these results, all of the models agree almost equally. However, a slight variance was noted in the fifth mode between the ANSYS and SubDyn models, which was due to the different ways ANSYS and SubDyn modeled the transition piece. With only one internal mode of the substructure, good approximation of the first nine modes of the entire system was achieved. As a result, the total DOFs were reduced by ~1,000. A comparison of Fig. 3 and Fig. 5 shows that the lowest modes are mostly associated with the tower, transition piece, and RNA (for the whole system). The number of retained substructure modes did not significantly affect the low-frequency modes of the entire structure.

Therefore, users may reliably limit the number of substructure modes and still obtain high-fidelity results for the whole system.

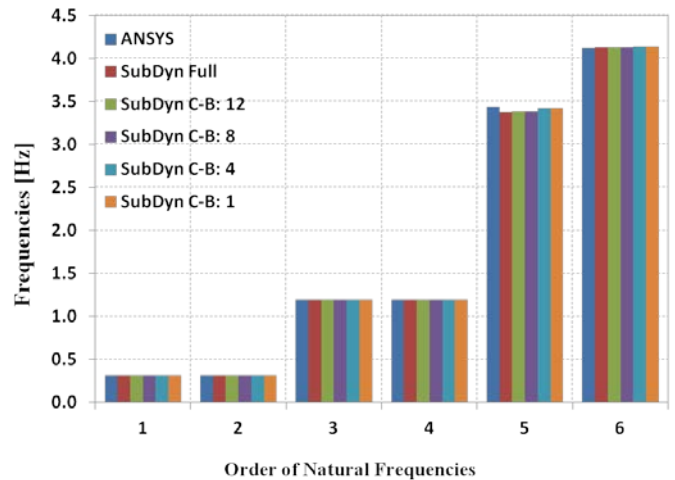


Fig. 5: Natural frequencies of the OC4 wind turbine system.

Table 4 and Table 5 show the x-direction deflections (see Fig. 4) calculated at the RNA center of mass and tower base, respectively, with thrusts applied at the RNA center of mass in the x-direction, which is the downwind direction. The thrust magnitude was arbitrarily varied between 2,000 kN and 4,000 kN, or approximately between the maximum expected thrust and a value that would cause yield in a limited region of the support structure. These results show that the outputs of SubDyn and ANSYS are very close, with small differences caused by the different ways that ANSYS and SubDyn model the transition piece (see Fig. 4). The number of internal modes used in the

SubDyn C-B model did not affect the deflection at the interface node or the static response of the tower and RNA. This outcome is to be expected because the Craig-Bampton method returns the exact static solutions at interface nodes via the restrained modes. Therefore, for the static analysis, the use of internal modes is not needed to achieve the correct solution for the entire turbine system.

Table 4. X-direction deflections at the RNA center of mass

Thrust at RNA [kN]	ANSYS [m]	SubDyn [m]				
		Full FEM	C-B: 12	C-B: 8	C-B: 4	C-B: 1
2000	1.2089	1.2084	1.2084	1.2084	1.2084	1.2084
4000	2.4178	2.4168	2.4168	2.4168	2.4168	2.4168

Table 5. X-direction deflections at the tower base

Thrust at RNA [kN]	ANSYS [m]	SubDyn [m]				
		Full FEM	C-B: 12	C-B: 8	C-B: 4	C-B: 1
2000	0.1375	0.1375	0.1375	0.1375	0.1375	0.1375
4000	0.2750	0.2750	0.2750	0.2750	0.2750	0.2750

CONCLUSIONS

This paper discussed recent upgrades made to FAST to enable loads simulations of offshore wind turbines with fixed-bottom, multimember support structures (e.g., jackets and tripods, which are commonly used in transitional-depth waters).

In particular, the main theory and strategies for implementing the multimember substructure structural-dynamics module (SubDyn) within the new FAST modularization framework were introduced. SubDyn relies on two main engineering schematizations: (1) a linear frame finite-element beam model (LFEB), and (2) a dynamics system reduction via Craig-Bampton’s method. The state-space formulation of SubDyn, which is important for time-domain simulations in the FAST framework, was also introduced.

The SubDyn LFEB can accommodate different element types, including Euler-Bernoulli and Timoshenko beam elements, either constant cross section or tapered. In this study, a Craig-Bampton system reduction was implemented to accelerate processing time while retaining a high level of fidelity in the overall system response. In general, the state-space formulation of the substructure equation of motion simplifies the time-domain calculation.

SubDyn can be used as a stand-alone module to perform modal analysis and analyze static response of multimember wind turbine substructures. In the future, SubDyn will be integrated into the FAST modularization framework through both loose and tight coupling and its full capabilities will therefore be available in a future release of FAST.

An example multimember support structure, the Offshore Code Comparison Collaboration Continuation (OC4) jacket, was analyzed using SubDyn and ANSYS. For all of the models, the modal analysis results were in agreement. Using only a few internal modes, the

SubDyn C-B models also revealed good results, which greatly reduces the number of degrees of freedom of the substructure. The second example showed the modal analysis and static response of an offshore system consisting of a National Renewable Energy Laboratory 5-megawatt wind turbine atop the OC4 substructure. The natural frequencies and the static deflections—under two different turbine rotor thrust levels—at the RNA center of mass and tower base, were calculated using SubDyn and ANSYS. The results revealed that the number of internal modes of the substructure had little effect on the lower-frequency modes of the entire wind turbine system. Therefore, limiting the number of internal modes will lead to relatively high-fidelity results, because the overall system dynamics are generally dominated by the low-frequency response. The static deflection at the RNA center of mass and tower base showed that the SubDyn results agreed with the ANSYS results, and the number of internal modes had no effect on the static response at the interface node, which was collocated at the transition piece reference point in this case (which had no effect on the tower and RNA either).

Based on the two example cases, the preliminary SubDyn results agreed with the ANSYS model outputs, thereby indicating that SubDyn, as a substructure module or a stand-alone code, may be considered as a reliable tool when analyzing multimember support structures for wind turbine systems.

ACKNOWLEDGMENTS

This work was performed at the National Renewable Energy Laboratory, in support of the U.S. Department of Energy (under contract #DEAC36-08GO28308).

REFERENCES

- Abdel-Jaber, MS, Al-Qaisia, AA, Beale, RG (2008). “Nonlinear natural frequencies of an elastically restrained tapered beam,” *J. Sound Vib.* 313:3–5, pp 772–783.
- ANSYS (2011). Mechanical/Emag, Release 14.0
- Craig, R, and Bampton, M (1968). “Coupling of Substructures for Dynamic Analyses.” *AIAA Journal*, Vol. 6, No.7, July 1968, pp 1313–1319.
- Damiani, R, Song, H, Robertson, A, Jonkman, J (2013a). “Assessing the Importance of Nonlinear Structural Characteristics in the Development of a Jacket Model for the Wind Turbine CAE Tool FAST.” *32nd International Conference on Ocean, Offshore and Arctic Engineering (OMAE2013)*, Nantes, France; June 9–14, 2013.
- Damiani, R, and Song, H (2013b). “A Jacket Sizing Tool for Offshore Wind Turbines within the Systems Engineering Initiative,” *Offshore Technology Conference*, Houston, TX, April 30–May 4, 2013.
- Das, D, Sahoo, P, Saha, K (2009). “Dynamic analysis of non-uniform taper bars in post-elastic regime under body force loading,” *Appl. Math. Model.* 33:11 (2009), pp 4163–4183.
- De Rosa, MA, Lippiello, M, Maurizi, MJ, Martin, HD (2010). “Free vibration of elastically restrained cantilever tapered beams with concentrated viscous damping and mass,” *Mech. Res. Commun.* 37:2 (2010), pp 261–264.

- Greenhill, LM, Bickford, WB, Nelson, HD (1985). "A Conical Beam Finite Element for Rotor Dynamics Analysis," *Journal of Vibration, Stress, and Reliability in Design*, Vol. 107.
- Hinnant, HE (1989). "Derivation of a Tapered p-Version Beam Finite Element," *NASA Technical Paper 2931, AVSCOM Technical Report 89-B-002*, August 1989.
- Hodges, DH, Ho, JC, Yu, W (2008). "The effect of taper on section constants for in-plane deformation of an isotropic strip," *Journal of Mechanics of Materials and Structures*. Vol. 3, No.3 (2008), pp 425–440.
- Hodges, DH, Rajagopal, A, Ho, JC, Yu, W (2010). "Stress and Strain Recovery for the In-plane Deformation of an Isotropic Tapered Strip-Beam," *Journal of Mechanics of Materials and Structures*, Vol. 5, No. 6, (2010), pp 963–975.
- Hurty, WC (1964). "On the Dynamic Analysis of Structural Systems Using Component Modes." *AIAA Paper No. 64-487, First AIAA Annual Meeting*, Washington, DC, June 29-July 2, 1964.
- Jonkman, JM (2007). "Dynamics Modeling and Loads Analysis of an Offshore Floating Wind Turbine," *Ph.D. Thesis. Department of Aerospace Engineering Sciences, University of Colorado, Boulder, CO, 2007; NREL/TP-500-41958*. Golden, CO: National Renewable Energy Laboratory.
- Jonkman, JM (2009). "Dynamics of Offshore Floating Wind Turbines—Model Development and Verification," *Wind Energy. Vol. 12, No. 5, July 2009, pp. 459-492; NREL/JA-500-45311*. Golden, CO: National Renewable Energy Laboratory; DOI: 10.1002/we.347.
- Jonkman, JM (2013a). "The New Modularization Framework for the FAST Wind Turbine CAE Tool," *51st AIAA Aerospace Sciences Meeting and 31st ASME Wind Energy Symposium*, Grapevine, TX.
- Jonkman, JM (2013b). FAST Theory Manual. *NREL/TP-500-32449*. Golden, CO: National Renewable Energy Laboratory (forthcoming).
- Jonkman, JM, and Buhl Jr., ML (2005). FAST User's Guide. *NREL/EL-500-38230*. Golden, CO: National Renewable Energy Laboratory.
- Laino, DJ and Hansen, AC (2002). User's Guide to the Wind Turbine Dynamics Aerodynamics Computer Software AeroDyn. Salt Lake City, UT: Windward Engineering LLC. *Prepared for the National Renewable Energy Laboratory under Subcontract No. TCX-9-29209-01*, December 2002.
- Moriarty, PJ, and Hansen, AC (2005). AeroDyn Theory Manual. *NREL/EL-500-36881*. Golden, CO: National Renewable Energy Laboratory, December 2005.
- Musial, W, and Ram, B (2010). "Large-Scale Offshore Wind Power in the United States: Assessment of Opportunities and Barriers." *NREL Report No. TP-500-40745*, 240 pp.
- Rao, SS, and Gupta, RS (2001). "Finite Element Vibration Analysis of Rotating Timoshenko Beams," *Journal of Sound and Vibration (2001)*, 242(1), pp 103–124.
- Song, H, Robertson, A, Jonkman, J, Sewell, DM (2012). "Incorporation of Multi-Member Substructure Capabilities in FAST for Analysis of Offshore Wind Turbines," *Offshore Technology Conference*, Houston, TX, April 30–May 4, 2012.
- Vemula, NK, DeVries, W, Fischer, T, Cordle, A, Schmidt, B (2010). "Design solution for the upwind reference offshore support structure." Upwind deliverable D4.2.6 (WP4: O_shore foundations and support structures), Ramb_II Wind Energy.
- Vorpahl, F, Kaufer, D, Popko, W (2011). Description of a Basic Model of the "Upwind Reference Jacket" for Code Comparison in the OC4 Project under IEA Wind Annex 30. Technical report, Fraunhofer Institute for Wind Energy and Energy System Technology IWES.